ELSEVIER

Journal of Molecular Catalysis B: Enzymatic 18 (2002) 99–108

JOURNAL OF MOLECULAR CATALYSIS B: ENZYMATIC

www.elsevier.com/locate/molcatb

Laccase-catalyzed oxidation of syringates in presence of albumins

Juozas Kulys [a,*], Kastis Krikstopaitis [a], Arturas Ziemys [b], Palle Schneider [c]

[a] *Institute of Biochemistry, Mokslininku 12, 2600 Vilnius, Lithuania*
[b] *Department of Biology, Faculty of Natural Sciences, Vytautas Magnus University, Vileikos 8, 3500 Kaunas, Lithuania*
[c] *Novozymes A/S, Smørmosevej 9, 2880 Bagsvaerd, Denmark*

Received 25 January 2002; accepted 27 May 2002

Abstract

Laccases-catalyzed oxidation of methyl syringate (MS) was investigated at pH 6.0 and 25 °C. The laccases used were recombinant *Polyporus pinsitus* laccase (rPpL) and recombinant *Myceliophthora thermophila* laccase (rMtL). The apparent Michaelis–Menten constant was 1.1 mM for rPpL and 3.6 mM for rMtL in air-saturated buffer solution. The bimolecular constants calculated as $k_{ox} = k_{cat}/K_m$ were 10.6 and 6.1 $(mM\,s)^{-1}$, respectively. During MS oxidation an inactivation of rMtL was indicated showing limited turnover capacity (TC) of the laccase. Human serum albumin (HSA) and bovine serum albumin (BSA) prevent laccase inactivation. Spectral measurements revealed MS complexation with albumins with dissociation constant 15.2 μM and 18.7 μM for BSA and HSA, respectively. Docking calculations showed that MS might complex within hydrophobic binding sites of albumins. The radical of MS formed during oxidation also binds within the same sites. The hypothesis was made that albumin is capable of trapping the radical preventing laccase inactivation.

Keywords: Laccase; Methyl syringate; Serum albumin; Kinetics; Binding constant; Docking

1. Introduction

During the last decade a huge amount of efforts have been made to apply laccases for various industrial processes such as delignification, dye or stain bleaching, water or soil remediation and waste waters detoxification [1–3]. To increase efficiency of these biocatalytical processes mediators are added [4,5]. Different organic redox compounds have been suggested as the mediators for laccase-catalyzed reactions [6–10]. A typical laccase substrate is syringic acid methyl ester (MS) [11,12]. MS is a natural product [13] and shows promising results as a laccase mediator due to a suitable redox potential. MS undergoes a single electron oxidation by laccase-catalyzed reaction and forms a phenoxy radical [11]. The scheme of MS-assisted target molecules conversion can be written as:

$$\text{laccase(ox)} + \text{MS} \rightarrow \text{laccase(red)} + \text{MS}^{\bullet} + \text{H}^{+} \quad (1)$$

$$\text{laccase(red)} + \text{O}_2 + 4\text{H}^{+} \rightarrow \text{laccase(ox)} + 2\text{H}_2\text{O} \quad (2)$$

$$\text{MS}^{\bullet} + \text{target molecule} + \text{H}^{+} \rightarrow \text{product} + \text{MS} \quad (3)$$

The yield of the mediator-assisted catalysis depends on the turnover capacity (TC) [14]. During investigation of laccase-catalyzed MS oxidation an inactivation of laccase has been observed resulting in limitation

Abbreviations: rPpL, recombinant *Polyporus pinsitus* laccase; rMtL, recombinant *Myceliophthora thermophila* laccase; HSA, human serum albumin; BSA, bovine serum albumin; MS, methyl syringate; ES, ethyl syringate; PS, propyl syringate

* Corresponding author. Tel.: +370-2-729176; fax: +370-2-729196.
E-mail address: jkulys@bchi.lt (J. Kulys).

1381-1177/02/$ – see front matter
PII: S1381-1177(02)00073-5

of TC. Moreover, it was noticed that some compounds, among them albumins, can prevent laccase inactivation and can increase the reaction yield. Since inactivation of oxidoreductases is a common phenomenon concomitant with oxidation of phenolic substances [15,16], the laccase inactivation during mediator oxidation is of general interest in these enzymes applications. Thus, finding the reasons for laccase inactivation may allow to improve the industrial processes in presence of mediators.

The task of this paper was to investigate kinetics of fungal laccases-catalyzed oxidation of MS with special emphasis on the mechanism of albumin as stabilizer.

2. Experimental

2.1. Materials

Recombinant *Polyporus pinsitus* laccase (rPpL) and recombinant *Myceliophthora thermophila* laccase (rMtL) heterologously expressed in *Aspergillus oryzae* were obtained from Novozymes A/S. Concentration of rPpL and rMtL was determined spectrophotometrically at 615 and 589 nm using an extinction coefficient 5.3 $(\text{mM cm})^{-1}$ [17] and 4.6 $(\text{mM cm})^{-1}$ [18], respectively. Recombinant laccases have the same pI, spectral properties, pH stability, specific activities and pH profiles as the native protein, and only specific activity of native MtL was lower than that of rMtL [17,19]. Methyl syringate (MS) from "Lancaster Synthesis" was additionally recrystallized from ethanol. Ethyl syringate (ES), propyl syringate (PS) were synthesized by Novozymes A/S, syringic acid was from "Aldrich". Solutions of MS, ES and PS were prepared by weight in methanol. Human serum albumin (HAS; purity 98%), and bovine serum albumin (BSA; purity 99%, fatty acids 0.1%) were from "Serva". The albumins were additionally pretreated to remove fatty acids, following procedure [20]. One gram of albumin was dissolved in 10 ml of distilled water. Activated charcoal (0.5 g) was added to the protein solution and mixed. The suspension was acidified to pH 3.0 by adding HCl. The mixture was placed in an ice bath and stirred magnetically for 1 h. Separation of charcoal from albumin was performed by centrifugation at 14.000 rpm for 20 min. The fresh protein solution was adjusted to pH 7.0 by the addition of NaOH and stored in refrigerator at 4 °C. The activated charcoal used was from ICN, Russia. Concentration of BSA and HSA was determined spectrophotometrically at 280 nm using an extinction coefficient 43.6 $(\text{mM cm})^{-1}$ [21] and 36.6 $(\text{mM cm})^{-1}$ [22], respectively. Chymotrypsinogen A (0.141% Intrinsic Chymo) was a product of Worthington Biochemical Corp., glucoamylase, bacterial α-amylase and insulin were all products of Novozymes A/S. Solutions of proteins were prepared by weight in buffer solution. The concentration of proteins was calculated according to the molecular weight taken from Fluka catalog, i.e. for chymotrypsinogen A 25 000 Da, glucoamylase 97 000 Da, α-amylase 58 000 Da and insulin 5733 Da.

2.2. Instruments, procedures and calculations

Oxygen consumption was measured in 10.0 ml thermostated cell by using a computer-controlled Clark-type oxygen electrode. The concentration of oxygen in the solution was assumed to be 0.25 mM. The reaction was carried out in 20 mM acetate buffer solution pH 6.0 at 25 °C. The initial steady-state rate was calculated by fitting the kinetic curves to third-order polynomial functions. The apparent Michaelis constant (K_m) and catalytic constant (k_{cat}) were calculated according to the Michaelis–Menten equation. An apparent bimolecular rate constant (k_{ox}) was stated as the ratio of k_{cat}/K_m. All data are presented as mean ± standard deviation.

Spectrophotometric measurements were performed by using a computer-controlled Gilford Instrument Lab spectrophotometer at 25 °C. A total of 20 mM acetate with pH 6.0, 20 mM citrate with pH 3.0 and 20 mM carbonate buffer with pH 10.0 were used as buffer solutions. To determine the complex formation of MS with albumin, the aliquots of 5–20 μl of stock solution containing 2 mM MS were added to the solution of proteins, the concentration of which changed in the range 10–50 μM. After mixing, the absorbance at 250–360 nm was recorded. The concentration of free syringate was calculated as difference of the initial and the complex bound syringate. The extinction coefficient of complexed syringate was calculated by extrapolating the absorbance at 330 nm to infinite BSA concentration. Dissociation constant of the complex was calculated by assuming that the albumin molecule

contains n equivalent binding centers and by using a non-linear model of the binding:

$$\frac{[MS]}{[MS]_0} = \frac{(1/2n[MS]_0 - 1/2nK_d - 1/2[Alb]_0 + 1/2n(K_d^2 + 2K_d[MS]_0 + 2K_d n[Alb]_0 + [MS]_0^2 - 2n[MS]_0[Alb]_0 + n^2[Alb]_0^2)^{1/2})n}{[MS]_0} \quad (4)$$

where $[MS]_0$ and $[MS]$ are the initial and uncomplexed concentration of MS, $[Alb]_0$ the initial albumin concentration and K_d the dissociation constant of the complex.

Ab initio calculations of MS structure and charges were performed on 3-21G basis set and Hartree-Fock theory with Gaussian 98W [23]. For docking simulations the rotation of methoxy groups, carboxymethoxy and hydroxyl group in MS and radical form were considered. The crystal data of native HSA (1AO6) and HSA structure with Myr and TIB was downloaded from Protein Data Bank [24,25]. Automated flexible docking simulations were performed by AutoDock 3.0.5 [26–28]. All non-protein compounds were removed from structures during MS docking calculations. Atomic interaction energy grid maps for HSA were calculated with 0.25 Å grid spacing and 120 grid points forming 30 Å cubic boxes centered on TIB binding pockets. The pocket in domain I was formed by Ile 142, His 146, Phe 149, Leu 154, Phe 157, Tyr 161, Arg 186, Gly 189 and Lys 190 and the pocket in domain II Lys 199, Leu 219, Phe 223, Leu 234, Leu 238, Val 241, His 242, Leu 260, Ala 261, Ile 264, Ile 290 and Ala 291. The space of the cubic boxes covered the binding pockets of HSA and the space beyond. The electrostatic interaction energy grid used a distance-dependent dielectric function of Mehler and Solmajer [29]. The docking was accomplished using Lamarckian genetic algorithm. The number of individuals in population was set up to 50. The maximum number of energy evaluations was 500 000 and maximum number of generation was 27 000. The number of the top individuals that are guaranteed to survive into the next generation was one. Crossover rate and mutation rate were 0.02 and 0.80, respectively. A total of 120 automated runs were calculated for each compound and for every binding pocket environment sets with cluster analysis. Cluster tolerance was set up to 1 Å. Local pseudo-Solis & Wets search was performed. The number of iterations for search was 300, and the probability of performing a local search on an individual was 0.06.

3. Results and discussion

3.1. Laccase-catalyzed oxidation of methyl syringate

The oxidation of MS catalyzed by rPpL showed typical Michaelis–Menten kinetics, as monitored by concomitant O_2 consumption (Fig. 1). The apparent K_m value was 1.1 ± 0.3 mM (Table 1).

The initial rate of rMtL-catalyzed MS oxidation reached steady-state level at larger MS concentration; an apparent K_m was determined to 3.6 ± 0.5 mM.

The kinetics of total oxygen consumption was different for the two laccases. In the case of rPpL the rate did not change up to 95% oxygen use (data not shown). In contrast, the oxygen consumption decreased if rMtL was used (Fig. 2). The rate indicated rMtL inactivation during the reaction. Inactivation of rMtL was dependent on the MS concentration. The inactivation was faster at higher MS concentration. During reaction of rMtL with MS the activity of the enzyme decreased up to 39% after 40 min. TC calculated as ratio of molar concentration of oxidized substrate to molar concentration of inactivated enzyme was 1025. Dialysis of inactivated laccase solutions against buffer did not restore the activity which showed the irreversible character of the inactivation of laccases during MS oxidation.

The addition of HSA to rMtL solution increased the total oxygen consumption (Fig. 2). At 50 μM of HSA

Table 1
Kinetic parameters of laccases-catalyzed MS oxidation determined from the initial rate of the reaction at pH 6.0

Laccase	HSA (μM)	K_m (mM)	k_{cat} (s^{-1})	k_{ox} ($(mM\,s)^{-1}$)
rPpL	–	1.1 ± 0.3	11.2 ± 1.0	10.6 ± 3.9
rPpL	10	0.4 ± 0.08	19.3 ± 1.0	47.1 ± 12.0
rMtL	–	3.6 ± 0.5	21.6 ± 1.3	6.1 ± 1.2
rMtL	10	9.6 ± 2.4	23.9 ± 3.7	2.5 ± 1.0
rMtL	50	11.2 ± 4.4	19.4 ± 5.0	1.7 ± 1.1

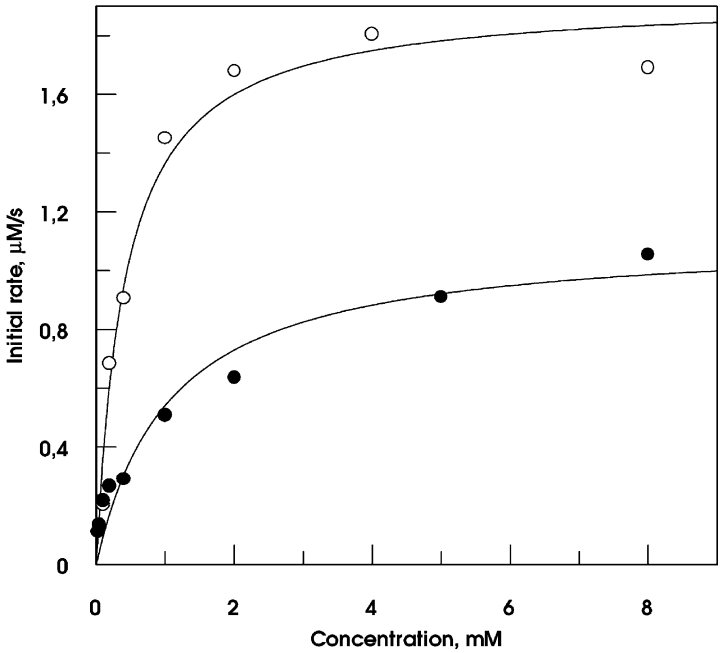

Fig. 1. The dependence of rPpL-catalyzed initial MS oxidation rate on substrate concentration in presence (○) and in absence of HSA (●): 20 mM acetate buffer, pH 6.0, 25 °C, 100 nM rPpL, 10 μM HSA.

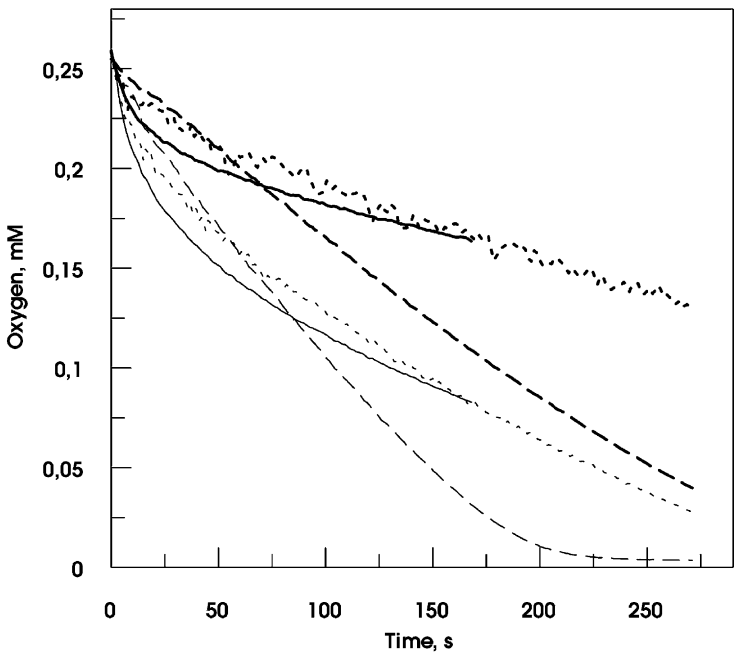

Fig. 2. Oxygen consumption during rMtL-catalyzed MS oxidation: 500 nM rMtL, 1 mM MS (solid bold), 1 mM MS and 10 μM HSA (dot bold), 1 mM MS and 50 μM HSA (broken bold), 2 mM MS (solid), 2 mM MS and 10 μM HSA (dot), 2 mM MS and 50 μM HSA (broken).

all oxygen was consumed during 4 min. The estimated TC was more than 10^4.

Inactivation of rPpL during oxidation of MS was much slower even in HSA-free solution. The enzyme activity decreased up to 71% after prolonged (2.5 h) incubation of the MS solution in the reactor. The calculated TC for rPpL was 10^5.

The addition of HSA into a rPpL-catalyzed process increased the initial rate of oxygen consumption, whereas in the case of rMtL the rate decreased (Fig. 2). This caused the changes of apparent K_m, k_{cat} and k_{ox}; k_{ox} increased for rPpL and decreased for rMtL (Table 1).

3.2. Spectra of methyl syringate during oxidation

At pH 6.0, solution of MS shows absorbance maximum at 274 nm. During MS incubation with rPpL, the absorbance shifted to longer wavelength (Fig. 3). This spectrum is a result of overlapping of two spectra. One spectrum belongs to MS and other may be attributed to the oxidized MS, i.e. to radical of MS that has a maximum of absorbance at 287 nm (Fig. 3). At beginning of the reaction 2 isosbestic points may be indicated at 258 and 280 nm. The decrease of absorbance during prolonged incubation indicated the splitting of the radical and the formation of a compound, with low absorbance at 287 nm. As such the compound possessing *o*-quinone structure may be suggested [11].

During rMtL-catalyzed MS oxidation the spectrum changed in different manner (Fig. 4). At beginning the decrease of absorbance at 274 and 287 nm may be observed. This can be explained by slower MS oxidation. Deconvolution of intermediate spectra also revealed two spectra corresponding to MS and its radical as in the case of rPpL-catalyzed process.

3.3. The absorption of syringates in presence of albumins

The addition of BSA to MS solution did not change the spectrum at pH 3.0 (Fig. 5). However, the

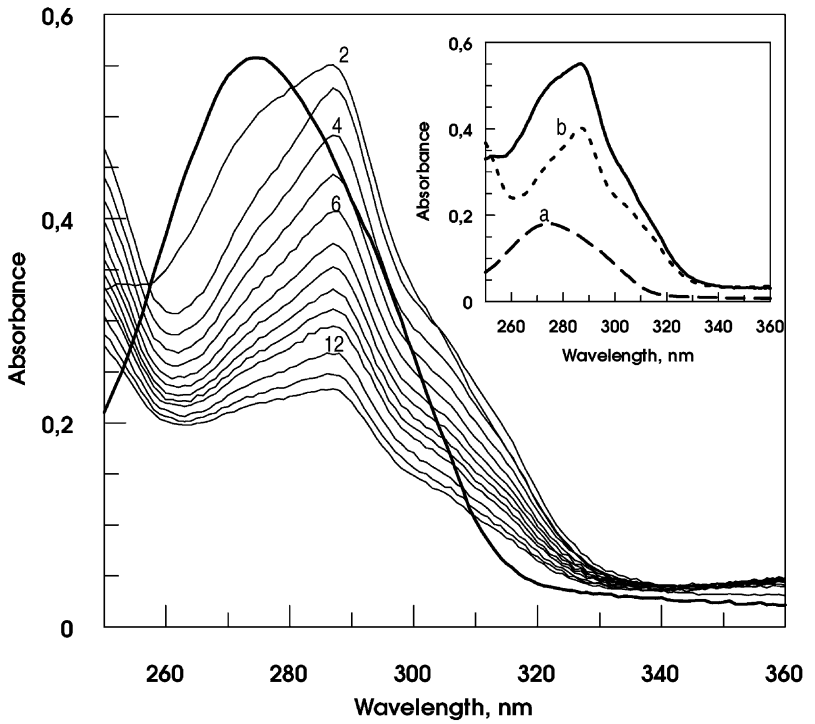

Fig. 3. The absorbance of MS (0.05 mM) in 20 mM acetate buffer, pH 6.0 (bold). The other spectra correspond to the reaction mixture obtained after addition of 46 nM rPpL. Spectra were recorded every 2.5 min (2–11) and 5 min (12–14). Inset shows the spectrum of intermediate at 5 min conversion: (a) MS, (b) MS radical.

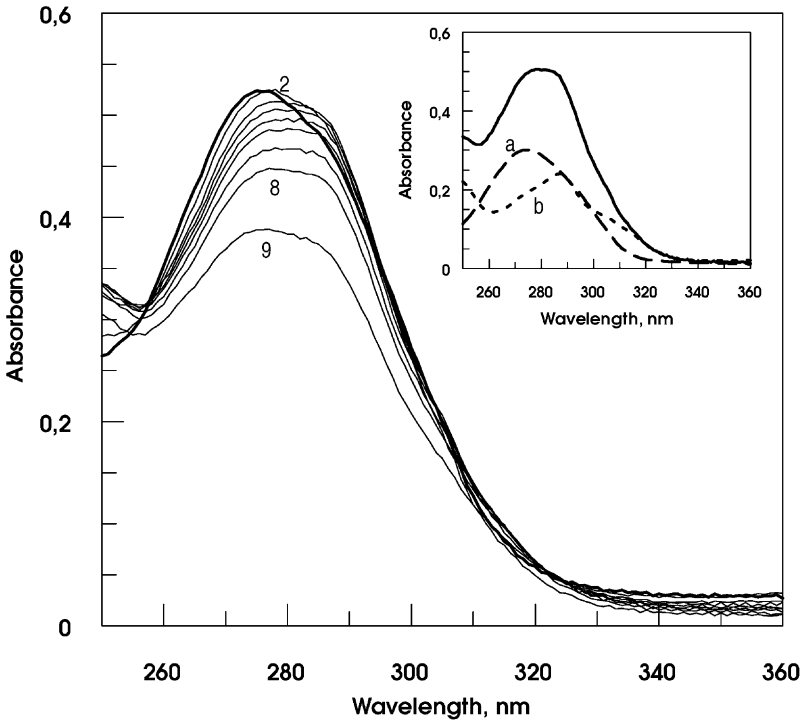

Fig. 4. The absorbance of MS (0.05 mM) in 20 mM acetate buffer, pH 6.0 (bold). The other spectra correspond to the reaction mixture obtained after addition of 415 nM rMtL. Spectra were recorded after every 2.5 min (2–6), 5 min (7), 10 min (8) and 20 min (9). Inset shows deconvolution of the spectrum of intermediate at 5 min conversion: (a) MS, (b) MS radical.

spectrum changed significantly at pH 6.0 with formation of new absorption band at 330 nm. At pH 10.0 BSA caused a small spectrum shift from 323 to 330 nm. Similar changes of the spectra were observed in presence of HSA for other syringate esters (ES, PS). At pH 6.0 ES and PS solutions with BSA showed new absorbance peak at 334 nm, and at pH 10.0 a small shift of absorbance maximum from 323 to 327 nm was indicated (Fig. 6).

To explain the absorbance changes, the spectra of pure MS solution was recorded at different pH. It was indicated that the spectra were the same at pH 3.0 and 6.0, but the peak shifted from 274 to 323 nm at pH 10 (Fig. 5).

MS spectrum changes in presence of albumins allowed to measure binding parameters. The titration of albumins solution with varied MS concentration gave $n = 1.06 \pm 0.04$ and 0.58 ± 0.01 for BSA and HSA, respectively. The calculated dissociation constants were 15.2 ± 5.4 and 18.7 ± 0.4 μM, respectively.

The control experiments of MS binding made by using other proteins at pH 6.0 showed that 10 μM of chymotrypsinogen A, glucoamylase, α-amylase or insulin did not show any absorbance increase of MS at 330 nm. At the same BSA concentration 17% of MS was complexed.

The spectrum changes during rMtL-catalyzed MS oxidation in presence of BSA are shown in Fig. 7. The absorbance at 330 nm decreased and absorbance at 265 nm increased during the reaction.

3.4. A scheme of albumin action

Kinetics of rMtL-catalyzed MS oxidation revealed inhibition of the reaction. The inhibition was irreversible since dialysis of inhibited rMtL did not restore the activity. TC calculated from experimental data (Fig. 1) was 1025. The constant oxygen consumption rate of the rPpL-catalyzed process and the larger TC may be explained by a higher resistance

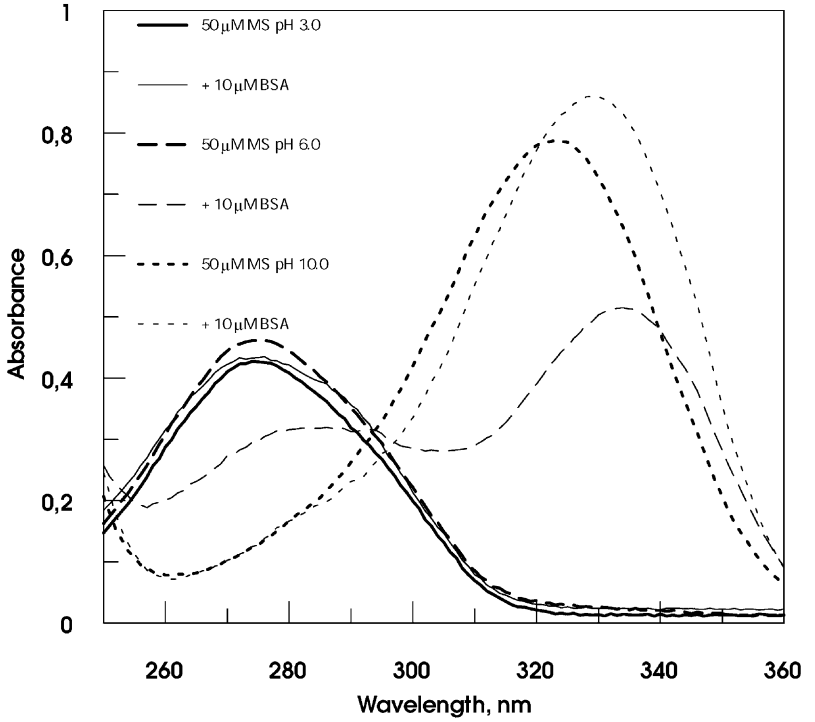

Fig. 5. The absorbance of MS at different pH and in presence of albumins: 0.05 mM MS (solid bold) with 0.01 mM BSA (solid) in 20 mM citrate buffer, pH 3.0; 0.05 mM MS (broken bold) with 0.01 mM BSA (broken) in 20 mM acetate buffer, pH 6.0; 0.05 mM MS (dot bold) and with 0.01 mM BSA (dot) in 20 mM carbonate buffer, pH 10.0.

to MS action. Calculations show that at TC more than 10^4 the inhibition could not been detected in the experimental scheme used.

Unexpected finding of this investigation was that albumins prevent laccase inhibition. To explain albumin action, the absorbance spectra of MS were analyzed in albumin free solution at different pH. The shifting of absorbance maximum to longer wavelength at alkaline pH must be attributed to MS dissociation:

$$\text{Ph–OH} \leftrightarrow \text{PhO}^- + \text{H}^+ \quad (5)$$

where Ph–OH corresponds to the non-dissociated form of MS.

PhO^- formed at alkaline pH and absorbed at longer wavelength in comparison to non-dissociated phenol [30]. In presence of albumins, however, the similar spectrum was generated at pH 6.0 (Figs. 5 and 6). This indicated that MS (ES) formed a complex with albumin and that MS in the complex was dissociated. In contrast to albumin other investigated proteins did not combine with MS. The albumins are known as fatty acids carriers in blood, but they also form a complex with aromatic compounds [31,32]. For example, HSA–myristate complex can bind two molecules of triiodobenzoic acid (TIB) [25]. The titration results of MS indicated that BSA can bind 1 mol of MS, whereas HSA binds 0.6 mol of MS. Since crystallographic data of HSA/TIB complex are available, the docking of MS in the albumin structure was performed. The calculation showed that MS may, indeed, form a complex in domains I and II of HSA in the same way as TIB [25]. The hydrophobic interaction is a main driving force of the complexes formation. In domain I the interaction of the phenol group with His 146 may be realized in addition. In domain II the phenolate group interacts with Lys 199 and His 242 (Fig. 8). Mean docking energy of the complex in domain I was −30.2 kJ/mol and in domain II −30.5 kJ/mol.

From docking calculations followed that HSA may combine more than 1 mol of MS. However, the

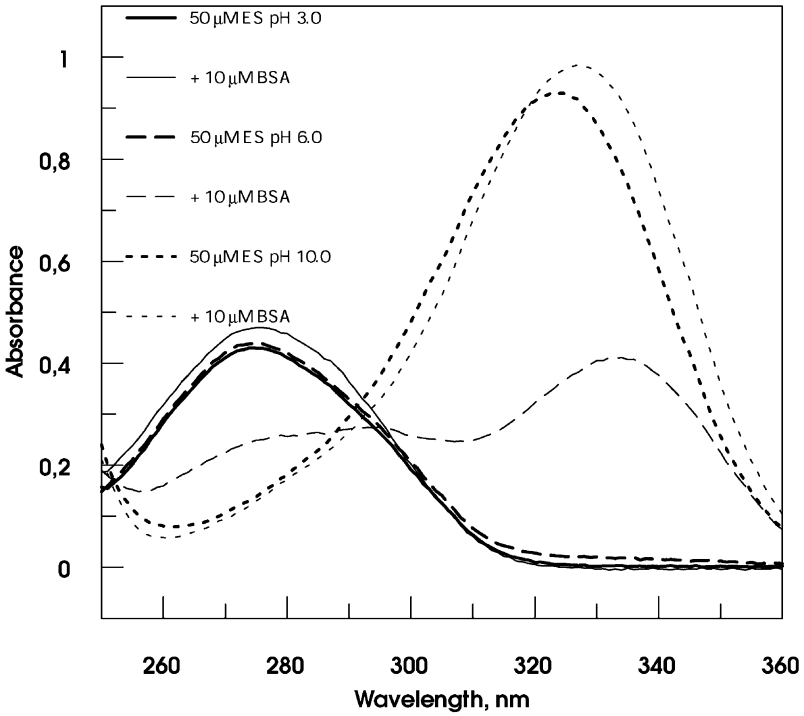

Fig. 6. The absorbance of ES at different pH and in presence of albumin: 0.05 mM ES (solid bold) with 0.01 mM BSA (solid) in 20 mM citrate buffer, pH 3.0; 0.05 mM ES (broken bold) with 0.01 mM BSA (broken) in 20 mM acetate buffer, pH 6.0; 0.05 mM ES (dot bold) and with 0.01 mM BSA (dot) in 20 mM carbonate buffer, pH 10.0.

titration indicated 0.6 mol of MS binding. This can be explained that calculations were performed with myristate/TIB structure of HSA, whereas experiment was performed with purified albumin. Fatty acids, as it was indicated in many publications, form the side of the aromatics complexation [25,33,34]. The amount of residual fatty acids, however, will vary for HSA and BSA. This may explain the difference of stoichiometry of HSA and BSA.

The binding of MS with albumins permits to explain albumins action on laccases-catalyzed MS oxidation. In literature, the mechanism of oxidoreductases inhibition is not completely clear, but suggestion was made that peroxidases inactivation in the presence of phenol substrates occurred by irreversible reactions between the enzyme and phenoxyl radicals formed by one electron oxidation of the phenol substrates during the catalytic cycle [15]. If this mechanism-based enzyme inactivation involving radical intermediates is valid for laccases, the action of albumins may be explained by radicals trapping. The calculations show that radical of MS may form the complexes with albumins in the same sites as MS. The docking energy of radical was very similar to MS, i.e. −29.3 and −30.0 kJ/mol for domains I and II of HSA, respectively. In contrast to MS, the complexation of the radical can be irreversible due to it fast reaction with polypeptide. The complexation and reaction of radicals with albumin will prevent laccases inactivation.

The low concentration of albumins used for retarding of laccases inactivation can not explain initial rate change due to decrease of free (unbound) MS concentration. Preliminary experiments show that laccases form complexes with albumins, and the complexation decreases activity of laccases. Therefore, the change of initial rate of MS oxidation might be associated with complex of albumin/laccase formation, rather than with MS concentration decrease.

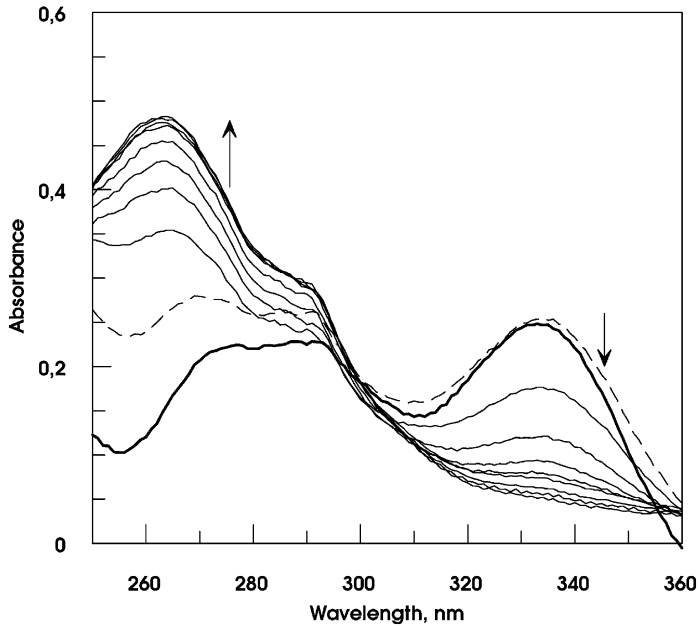

Fig. 7. Absorbance change during rMtL-catalyzed MS oxidation in presence of BSA solution at pH 6.0; 20 mM acetate buffer, 415 nM rMtL, 0.05 mM MS, 0.01 mM BSA. Solid bold curve shows initial absorbance of MS and BSA solution, the arrows indicate the directions of change in absorbance.

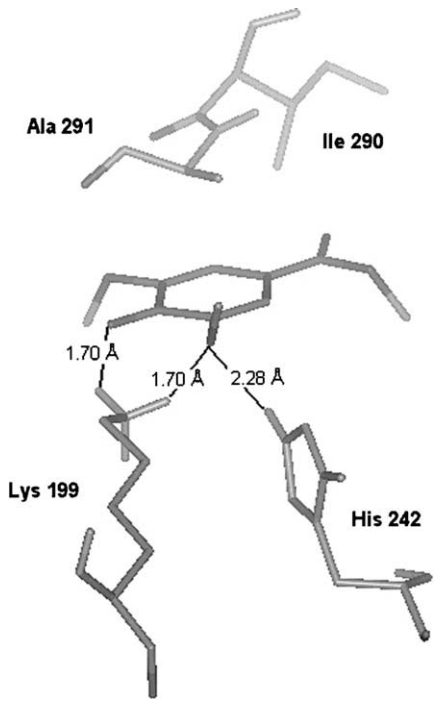

Fig. 8. The docking of MS in the domain II of HSA.

References

[1] J.-M. Bollag, K.L. Shuttleworth, D.H. Anderson, Appl. Environ. Microbiol. 53 (1988) 3086.
[2] H.P. Call, I. Mücke, J. Biotechnol. 40 (1997) 163.
[3] L. Gianfreda, F. Xu, J.-M. Bollag, Bioremedation J. 3 (1999) 1.
[4] R. Bourbonnais, M.G. Paice, FEBS Lett. 267 (1990) 99.
[5] P. Schneider, A.H. Pedersen, World patent application WO 95/01426 (1995).
[6] F. Xu, W. Shin, S.H. Brown, J.A. Wahleithner, U.M. Sundaram, E.I. Solomon, Biochim. Biophys. Acta 1292 (1996) 303.
[7] F. Xu, Biochemistry 35 (1996) 7608.
[8] K. Li, F. Xu, K.-E.L. Eriksson, Appl. Environ. Microbiol. 65 (1999) 2654.
[9] F. Xu, J. Kulys, K. Duke, K. Li, K. Krikstopaitis, H.-J. Deussen, E. Abbate, V. Galinyte, P. Schneider, Appl. Environ. Microbiol. 66 (2000) 2052.
[10] J. Kulys, K. Krikstopaitis, A. Ziemys, J. Biol. Inorg. Chem. 5 (2000) 333.
[11] V. Ducros, A.M. Brzozowski, K.S. Wilson, S.H. Brown, P.R. Østergaard, P. Schneider, D.S. Yaver, A.H. Pedersen, G.J. Davies, Nat. Struct. Biol. 5 (1998) 310.
[12] P. Schneider, M.B. Caspersen, K. Mondorf, T. Halkier, L.K. Skov, P.R. Østergaard, K.M. Brown, S.H. Brown, F. Xu, Enzyme Microbiol. Technol. 25 (1999) 502.
[13] R.J. Weston, K.R. Mitchell, K.L. Allen, Food Chem. 64 (1999) 295.

[14] M.D. Aitken, P.E. Heck, Biotechnol. Prog. 14 (1998) 487.
[15] K.J. Baynton, J.K. Bewtra, N. Biswas, K.E. Taylor, Biochim. Biophys. Acta 1206 (1994) 272.
[16] S. Gaspard, E. Monzani, L. Casella, M. Gullotti, S. Maritano, A. Marchesini, Biochemistry 36 (1997) 4852.
[17] D.S. Yaver, F. Xu, E.J. Golightly, K.M. Brown, S.H. Brown, M.W. Rey, P. Schneider, T. Halkier, K. Mondorf, H. Dalbøge, Appl. Environ. Microbiol. 62 (1996) 834.
[18] F. Xu, R.M. Berka, J.A. Wahleithner, B.A. Nelson, J.R. Shuster, S.H. Brown, A.E. Palmer, E.I. Solomon, Biochem. J. 334 (1998) 63.
[19] P.M. Berka, P. Schneider, E.J. Golightly, S.H. Brown, M. Madden, K.M. Brown, T. Halkier, K. Mondorf, F. Xu, Appl. Environ. Microbiol. 63 (1997) 3151.
[20] R.F. Chen, J. Biol. Chem. 242 (1967) 173.
[21] D.B. Wetlaufer, Adv. Protein Chem. 17 (1962) 378.
[22] M.J. Hunter, F.C. McDuffie, J. Am. Chem. Soc. 81 (1959) 1400.
[23] M.J. Frisch, G.W. Trucks, H.B. Schlegel, P.M.W. Gill, B.G. Johnson, M.A. Robb, J.R. Cheeseman, T. Keith, G.A. Petersson, J.A. Montgomery, K. Raghavachari, M.A. Al-Laham, V.G. Zakrzewski, J.V. Ortiz, J.B. Foresman, J. Cioslowski, B.B. Stefanov, A. Nanayakkara, M. Challacombe, C.Y. Peng, P.Y. Ayala, W. Chen, M.W. Wong, J.L. Andres, E.S. Replogle, R. Gomperts, R.L. Martin, D.J. Fox, J.S. Binkley, D.J. Defrees, J. Baker, J.P. Stewart, M. Head-Gordon, C. Gonzalez, J.A. Pople, Gaussian 94, Revision E.1, Gaussian Inc., Pittsburgh, PA, 1995.
[24] S. Sugio, A. Kashima, S. Mochizuki, M. Noda, K. Kobayashi, Protein Eng. 12 (1999) 439.
[25] S. Curry, H. Mandelkow, P. Brick, N. Franks, Nat. Struct. Biol. 5 (1998) 827.
[26] D.S. Goodsell, A.J. Olson, Proteins: Struct., Funct., Genet. 8 (1990) 195.
[27] G.M. Morris, D.S. Goodsell, R. Huey, A.J. Olson, J. Com. Aid. Mol. Des. 10 (1996) 293.
[28] G.M. Morris, D.S. Goodsell, R.S. Halliday, R. Huey, W.E. Hart, R.K. Belew, A.J. Olson, J. Comput. Chem. 19 (1998) 1639.
[29] E.L. Mehler, T. Solmajer, Protein Eng. 4 (1991) 903.
[30] R.F. Chen, Extrinsic and intrinsic fluorescence in study of protein structure: a review, in: G.G. Guilbault (Ed.), Fluorescence, Theory, Instrumentation, and Practice, Marcel Dekker, New York, 1967, p. 443.
[31] D.C. Carter, J.X. Ho, Adv. Protein Chem. 45 (1994) 152.
[32] X.M. He, D.C. Carter, Nature 358 (1992) 209.
[33] H. Vorum, B. Honoré, J. Pharm. Pharmacol. 48 (1996) 870.
[34] A.A. Bhattacharya, T. Grüde, S. Curry, J. Mol. Biol. 303 (2000) 721.